International Journal of Microwave and Wireless Technologies

cambridge.org/mrf

Feather-shaped super wideband MIMO antenna

Sarthak Singhal

Department of Electronics & Communication Engineering, Malaviya National Institute of Technology, Jaipur, Rajasthan 302017, India

Research Paper

Cite this article: Singhal S (2021). Feather-shaped super wideband MIMO antenna. *International Journal of Microwave and Wireless Technologies* **13**, 94–102. https://doi.org/10.1017/S1759078720000549

Received: 25 November 2019
Revised: 16 April 2020
Accepted: 18 April 2020
First published online: 19 May 2020

Key words:
Feather shaped monopole; multiple input multiple output antenna; coplanar waveguide feeding; super wideband applications

Author for correspondence:
Sarthak Singhal,
E-mail: sarthak.ece@mnit.ac.in

Abstract

Two configurations of a modified feather-shaped antenna element are proposed for super wideband (SWB) multiple-input multiple-output (MIMO) applications. The antenna element geometry comprises of a circular slot-loaded feather-shaped radiator and rectangular notch-loaded quarter elliptical coplanar waveguide ground plane. An operating bandwidth of 4.4–51.5 GHz with inter-port isolation, $S_{21} \geq 15$ dB for spatial diversity configuration, and 3.8–51.5 GHz with $S_{21} \geq 15$ dB in pattern diversity configuration are achieved. The footprints of the antenna configurations are 17×33 and 31×31 mm^2. Both configurations exhibited an envelope correlation coefficient of <-20 dB. The proposed MIMO configurations are fabricated and experimentally validated. The designed antenna configurations are SWB and compact.

Introduction

During the past few years, the demands for wireless high data rate over multibands/wideband frequency spectrum have increased significantly. To fulfill these demands, the frequency spectrum 3.1–10.6 GHz is allocated to ultrawideband (UWB) applications for unlicensed usage in 2002. This approval stimulated the interest for investigating wideband antenna structures fulfilling these demands. The approved frequency spectrum covered only the short-range communication services but not the long-range communication range. To fulfill both frequency spectrums, i.e. long-range and short-range communication services, the term super wideband (SWB) technology was coined. A technology having ratio bandwidth of ≥10:1 is defined as SWB technology. Few planar antenna geometries having miniaturized dimensions and super wide bandwidth are already proposed.

Another challenge for these wideband wireless antenna structures is the mitigation of fading effects in multipath environments. These signal fading effects are mitigated by integrating the multiple-input multiple-output (MIMO) technology with UWB/SWB antenna structures. This integration led to an increase in the channel capacity. MIMO technology uses multiple uncorrelated antenna structures for transmission and reception purpose. Few wideband MIMO antenna structures are already available in the literature [1–24]. These reported structures included both spatial (i.e. same radiation patterns) and pattern (i.e. different radiation patterns) diversity configurations. In most of these MIMO configurations, the inter-port isolation between the two ports is enhanced by using various decoupling structures which include grounded stubs, neutralization lines, inter-digital structures, diagonal structures, etc.

From the available literature, it is observed that the previously reported structures have either large dimensions or bandwidth unable to cover UWB frequency spectrum or beyond it. In the available literature, antenna designers [24–33] have used FR-4 epoxy substrate due to its low cost. On the other side, some researchers have avoided it due to its losses at millimeter range frequencies [34, 35].

In this paper, two diversity antenna configurations, i.e. spatial and pattern that are of a feather-shaped SWB antenna, are presented. The feather-shaped radiating patch is designed by using multiple rotated elliptical monopoles. The bandwidth is enhanced by using the techniques of circular slot loading of the radiating patch, modified quarter elliptical coplanar waveguide (CPW) ground planes, and rectangular notch loading of the ground plane. The isolation in spatial diversity configuration is enhanced by placing two antenna elements in coplanar manner with a distance of $\lambda/10$ between the two radiating elements. The isolation between the two orthogonal antenna elements in pattern diversity configuration is enhanced by using a diagonal metallic strip. The single antenna element and both diversity configurations are designed and analyzed by using FEM-based Ansoft's HFSS Simulator.

Antenna design

The optimized antenna configurations are presented in Fig. 1. The material used as a substrate in both configurations is 1.6 mm-thick FR-4 epoxy. The feather-shaped monopole comprises of 11 rotated elliptical radiators. This monopole is fed by conventional rectangular microstrip

© Cambridge University Press and the European Microwave Association 2020

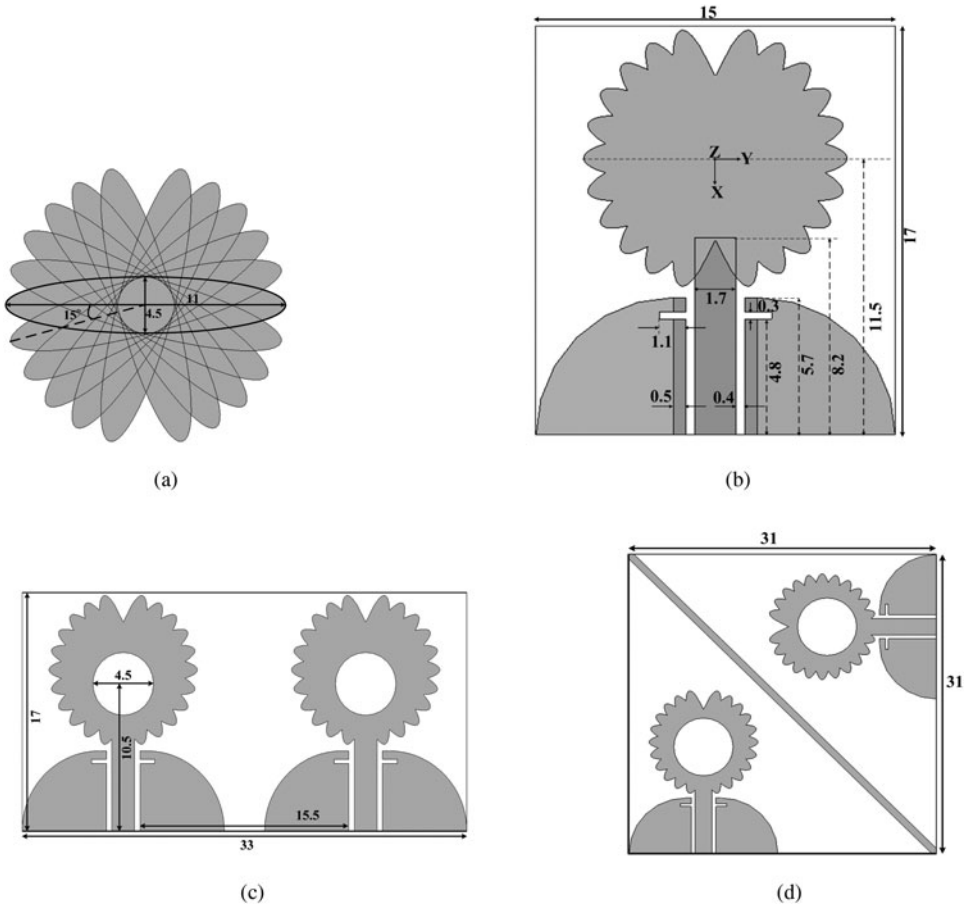


Fig. 1. Antenna configurations. (a) Radiating patch. (b) Single antenna. Spatial diversity configuration (Ant I). Pattern diversity configuration (Ant II).

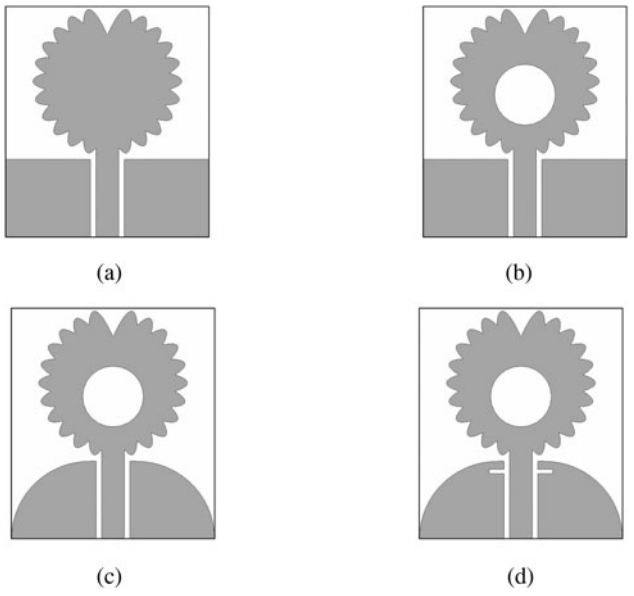


Fig. 2. Antenna element design steps. (a) Without central slot. (b) Conventional partial ground plane. (c) Without ground notches. (d) Proposed antenna.

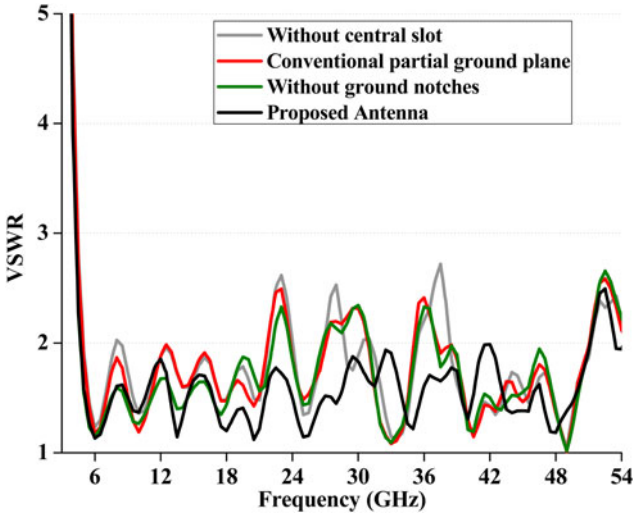


Fig. 3. VSWR characteristics for intermediate antenna element design stages.

feedline designed according to antenna design equations. A central circular slot is loaded on the radiator geometry to enhance the bandwidth by improving impedance matching. Thereafter, a pair of rectangular notches is loaded on the modified CPW ground plane to further improve the impedance matching and enhance the overall impedance bandwidth. The ground plane comprises of quarter elliptical and rectangular metallic sections. The antenna element design steps are demonstrated in Fig. 2. During the systematic optimization of antenna dimensions, one dimension is varied while keeping all other dimensions fixed.

https://doi.org/10.1017/S1759078720000549 Published online by Cambridge University Press

Table 1. Comparison of antenna element design stages

Bands	Without central slot	Conventional partial ground plane	Without ground notches	Proposed Antenna
Band 1 (GHz)	4.7–8.3	4.7–22.1	4.4–22.6	4.4–51.5
Band 2 (GHz)	8–22.2	23.6–27.4	23.5–27.1	–
Band 3 (GHz)	23.8–27.2	30.6–35.4	30.8–35.6	–
Band 4 (GHz)	28.5–30.8	37–51.4	36.8–51.5	–
Band 5 (GHz)	30.9–35.7	–	–	–
Band 6 (GHz)	38.1–51.6	–	–	–

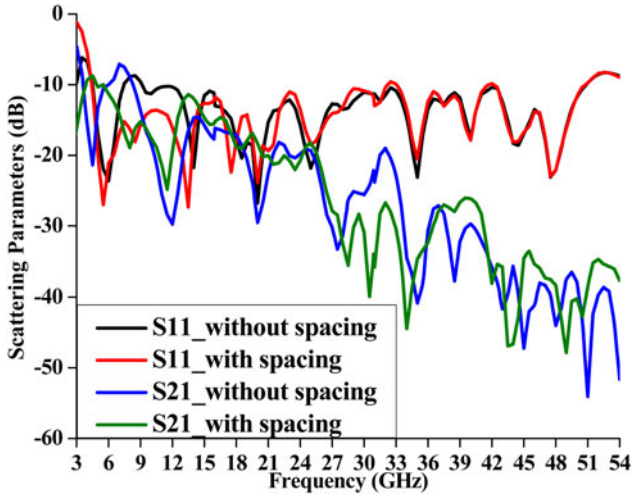


Fig. 4. Scattering parameters of spatial diversity configuration with variations in inter-element spacing.

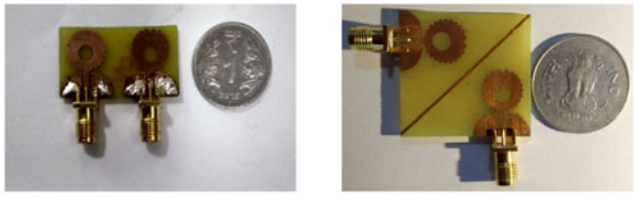


Fig. 5. MIMO antenna prototypes. (a) Spatial diversity. (b) Pattern diversity.

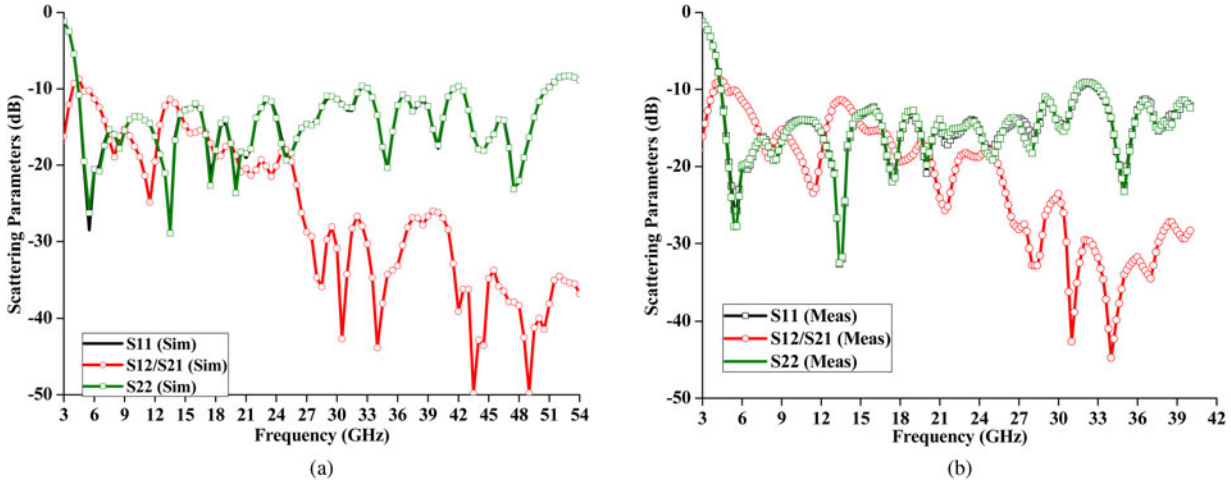


Fig. 6. Scattering parameters of spatial diversity antenna configuration. (a) Simulated. (b) Measured.

In spatial diversity configuration, two elements are arranged on the same side of the substrate with a fixed distance of $\lambda/10$ between the radiating patches without any additional decoupling structure. For pattern diversity configuration, two identical antenna elements are arranged orthogonally with a distance of 3 mm between their radiating elements and a 1 mm-thick metallic strip is placed diagonally across the substrate and coplanar with the antenna geometries.

Results and discussion

The intermediate antenna element designs are compared in terms of their VSWR characteristics and operating bands in Fig. 3 and Table 1, respectively. It is observed that six operating bands are achieved for antenna without central slot. The central slot loading resulted into the merging of the first two operating bands of above antenna and removal of the fourth operating band with no significant effect on remaining bands. The replacement of rectangular ground plane with modified quarter-elliptical ground plane resulted in bandwidth enhancement for the first and last operating bands of the previous antenna. The loading of the ground plane with rectangular notches resulted in the merging of all operating bands into a single SWB.

Frequency domain results

Spatial diversity configuration

The scattering parameters of spatial configuration with variations in inter-element spacing are presented in Fig. 4. It is observed that the reflection coefficient and isolation improved with an increase in inter-element spacing from 0 to 2 mm.

The MIMO antenna prototypes are presented in Fig. 5. Due to the limitation of available facilities, measurements up to only 40 GHz can be carried out. The variations of scattering parameters with respect to the frequency obtained from HFSS and experimental measurement are illustrated in Fig. 6. The discrepancies between the simulated and experimental results are due to fabrication and soldering errors. Due to the identical antenna elements, this MIMO antenna configuration is a symmetrical network. This symmetry in network leads to equal input impedance at both excitation ports of this MIMO antenna configuration. This impedance equivalence leads to equivalence in reflection coefficient, i.e. $S_{11} = S_{22}$. The couplings or isolation

https://doi.org/10.1017/S1759078720000549 Published online by Cambridge University Press

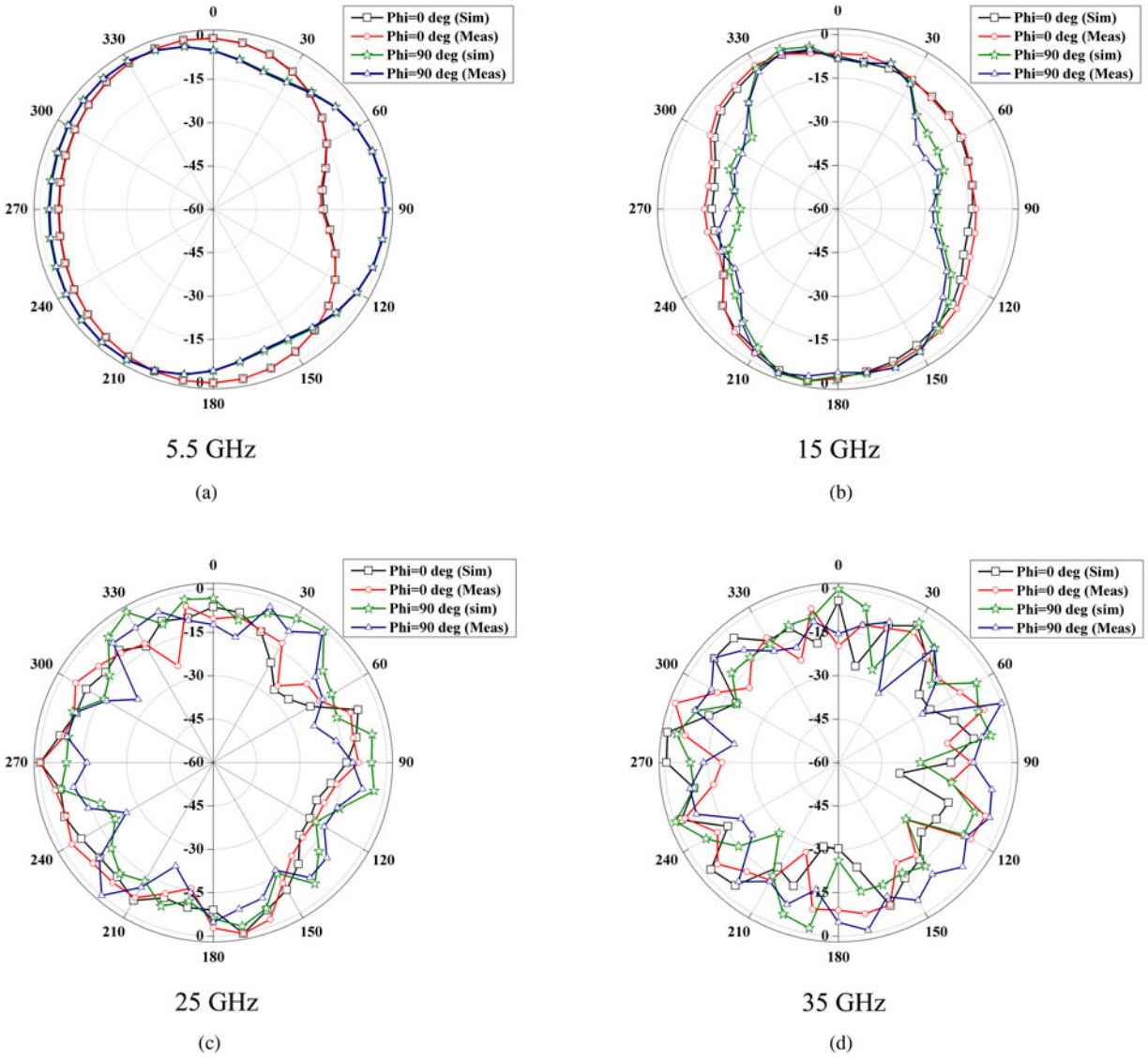


Fig. 7. Radiation patterns of spatial diversity antenna configuration. (a) 5.5 GHz. (b) 15 GHz. (c) 25 GHz. (d) 35 GHz.

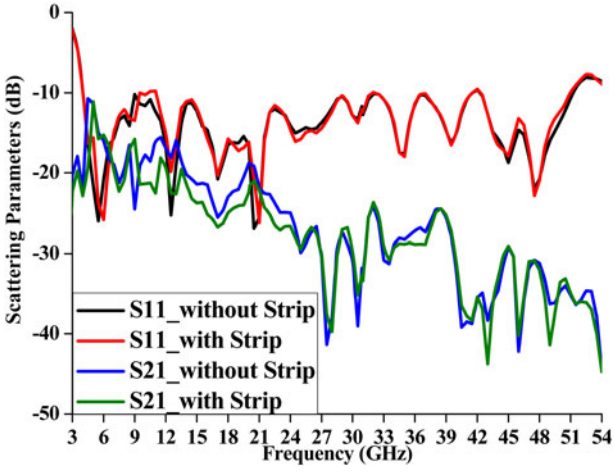


Fig. 8. Scattering parameters of pattern diversity configuration with and without diagonal strip.

plots are identical, i.e. $S_{21} = S_{12}$ because the two-port network is passive and hence reciprocal. Figure 6 demonstrates that both elements have an operating bandwidth (for VSWR ≤ 2) of 4.4–51.5 GHz (~11:1). In addition to this, isolation (S_{21} or S_{12}) $\geq$15 dB at maximum operating frequencies in the operating band is observed. This isolation fulfills the requirement of MIMO applications.

Figure 7 presents that bidirectional and omnidirectional patterns in *E*-plane and *H*-plane are achieved at frequencies <10 GHz for both elements. Similarly for frequencies >10 GHz, the patterns acquired distorted omnidirectional nature due to excitation of higher order modes.

Pattern diversity configuration

Figure 8 displays the effect of diagonal strip on the pattern diversity configuration performance. It is observed that the reflection coefficient is unaffected, whereas the inter-element isolation is improved with the introduction of diagonal strip between the elements.

https://doi.org/10.1017/S1759078720000549 Published online by Cambridge University Press

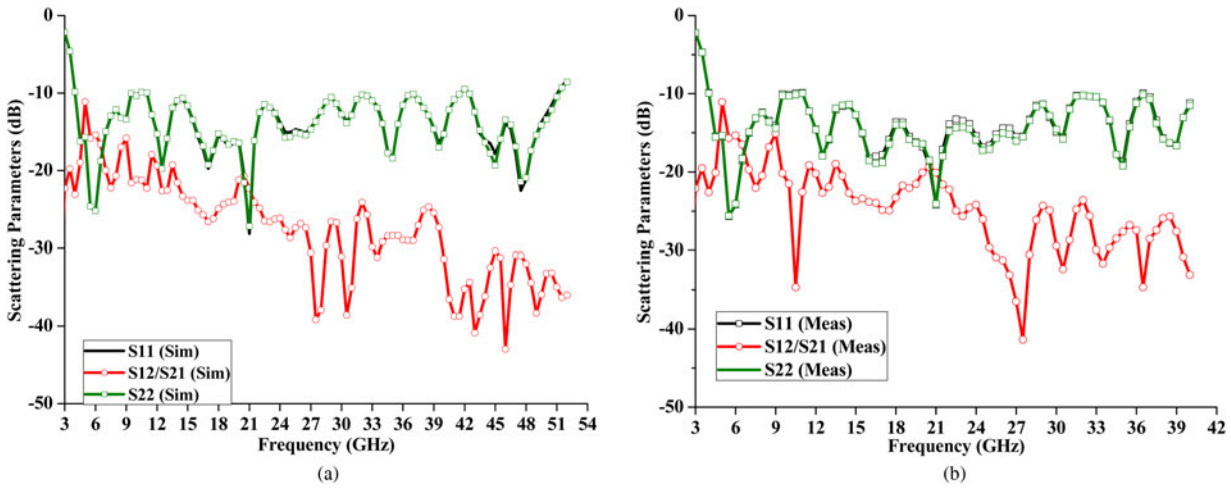


Fig. 9. Scattering parameters of pattern diversity antenna configuration. (a) Simulated. (b) Measured.

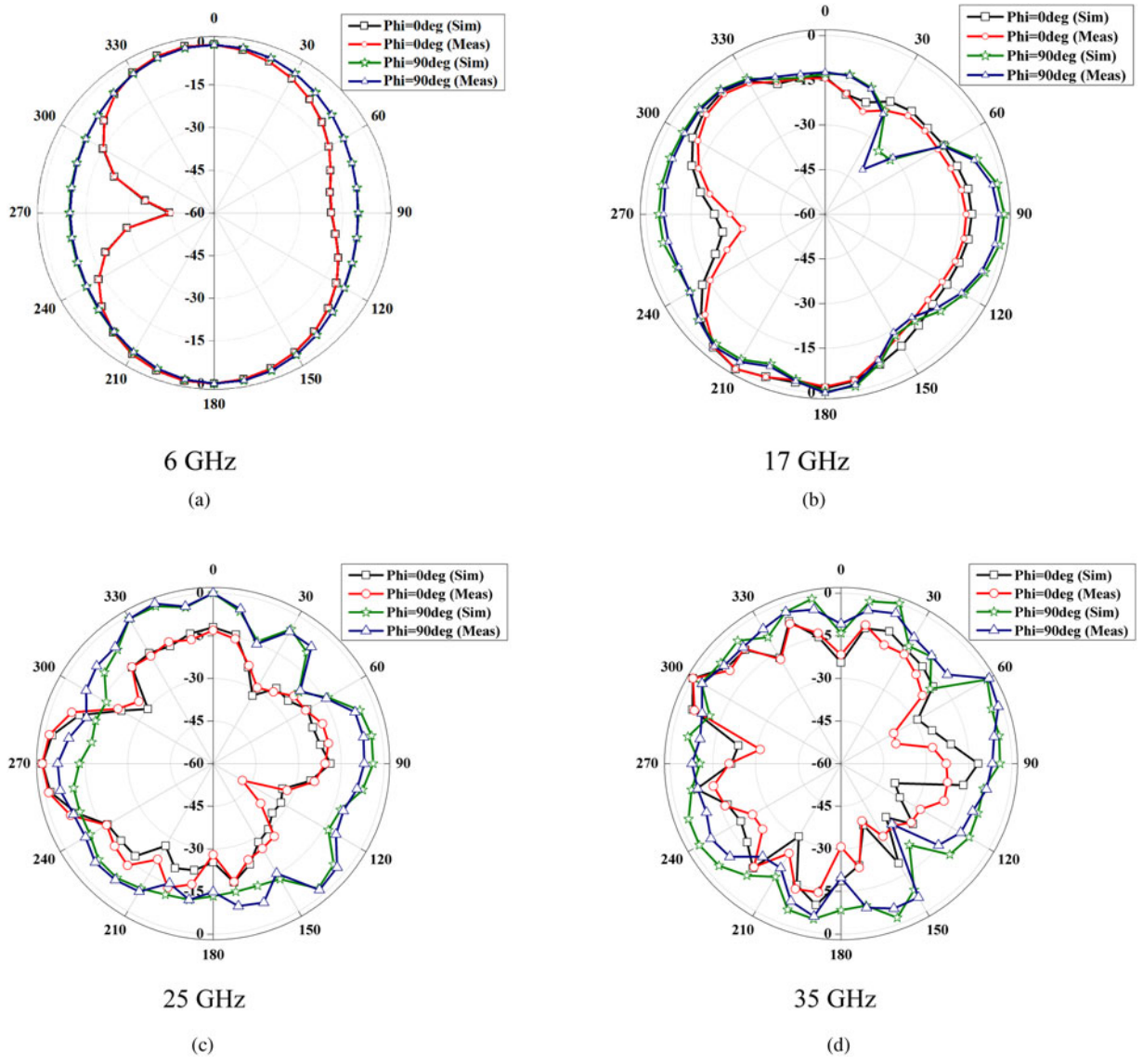


Fig. 10. Radiation patterns of pattern diversity antenna configuration for Port 1. (a) 6 GHz. (b) 17 GHz. (c) 25 GHz. (d) 35 GHz.

https://doi.org/10.1017/S1759078720000549 Published online by Cambridge University Press

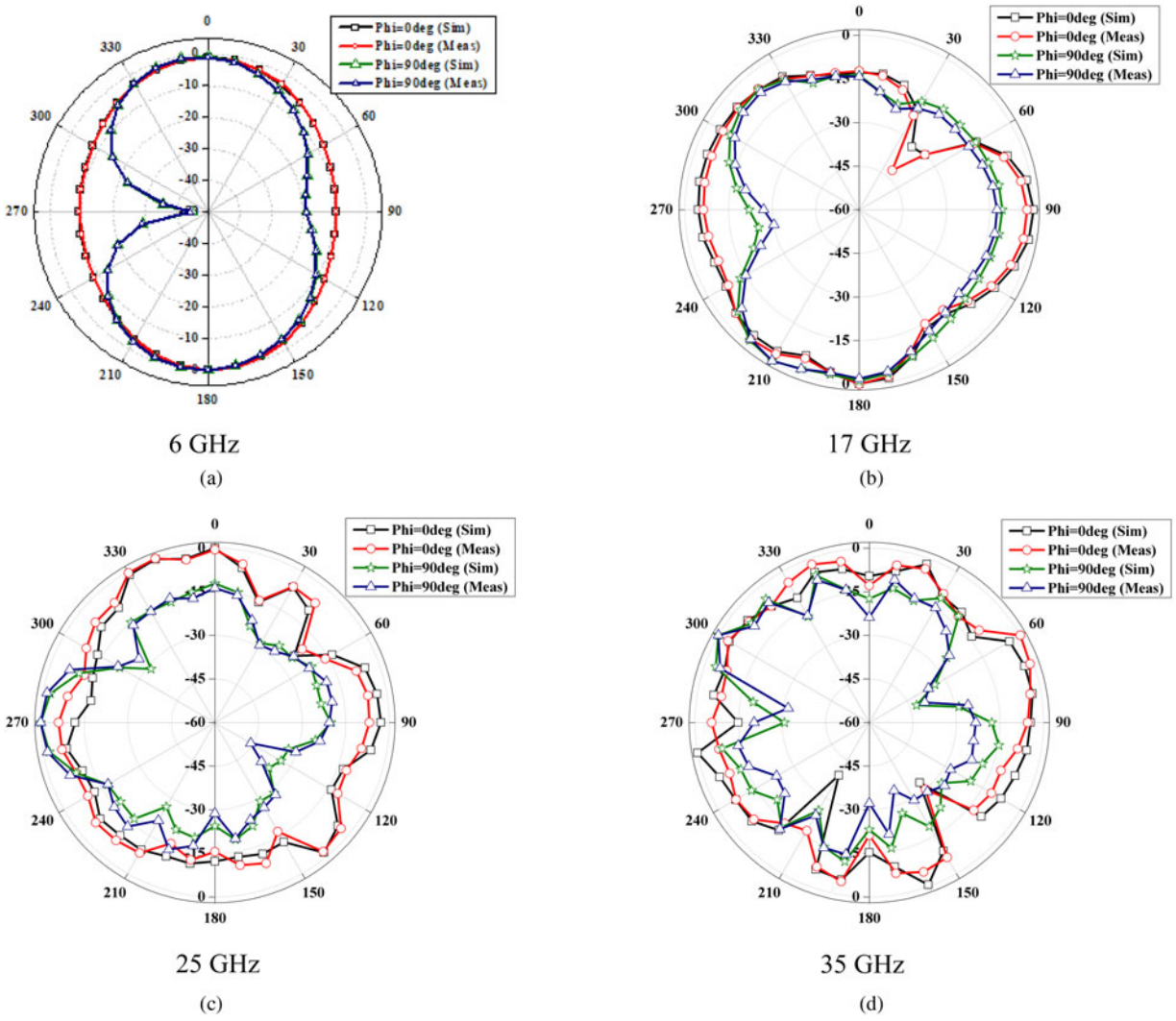


Fig. 11. Radiation patterns of pattern diversity antenna configuration for Port 2. (a) 6 GHz. (b) 17 GHz. (c) 25 GHz. (d) 35 GHz.

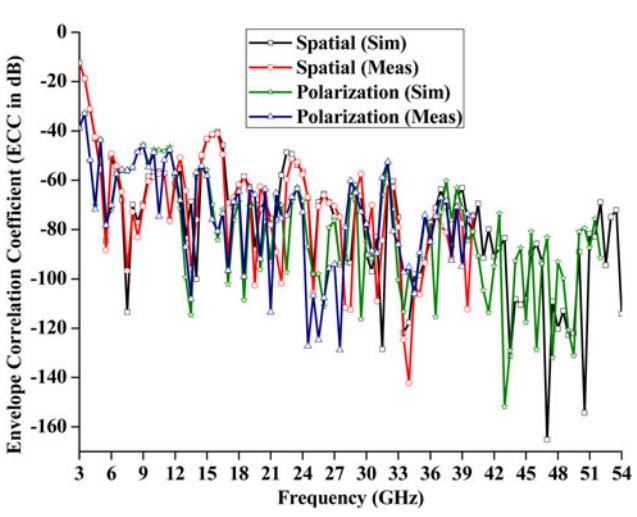


Fig. 12. Envelope correlation coefficient for two MIMO configurations.

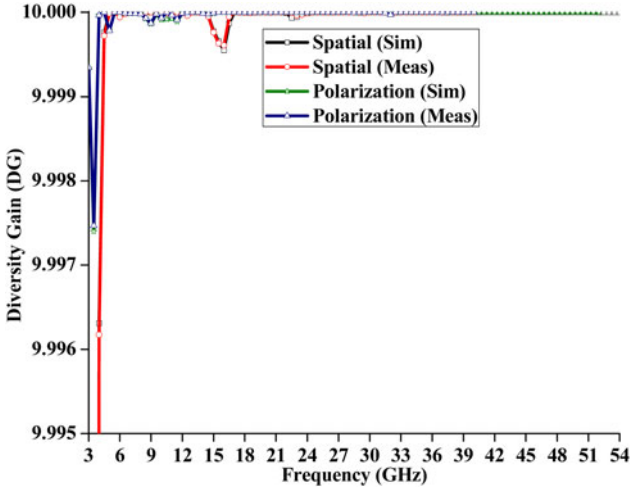


Fig. 13. Diversity gain variations with frequency for two MIMO antenna configurations.

https://doi.org/10.1017/S1759078720000549 Published online by Cambridge University Press

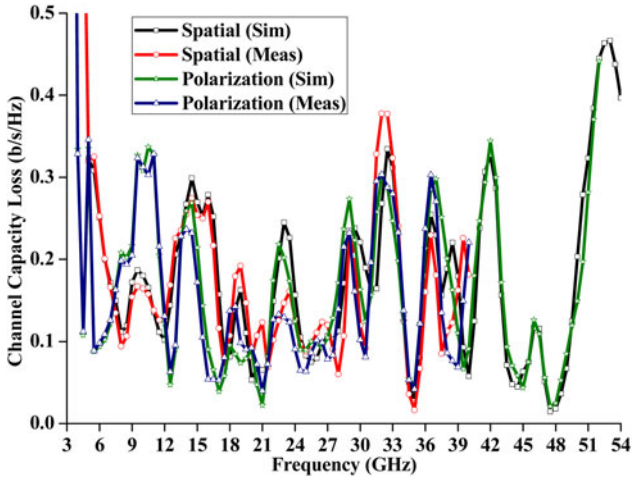


Fig. 14. Channel capacity loss for two MIMO configurations.

Since the antenna elements are identical, equal input impedance is observed for both ports leading to equal reflection coefficients ($S_{11} = S_{22}$) and isolation values ($S_{12} = S_{21}$). Figure 9 illustrates that each element has an operating bandwidth of 3.8–51.5 GHz (~13:1). Except at the frequency of 5 GHz ($S_{21} = S_{12} = 11$ dB), the inter-port isolation≥15dB is achieved. The isolation is increasing with frequency. A maximum isolation of 43 dB is achieved. These values of inter-port isolation present a very low level after considering the extreme bandwidth and miniaturized antenna dimensions.

Figures 10 and 11 present the radiation patterns of both elements at some frequency points in both planes. It is observed that the patterns are bidirectional and omnidirectional for frequencies <10 GHz. For higher frequencies, distorted omnidirectional patterns are observed in both planes. The patterns of element 2 are found to be orthogonal to those of element 1 at lower frequencies. In case of higher frequencies, due to the distorted omnidirectional nature, the 90° phase shift in patterns is not easily recognizable.

Diversity performance

The effectiveness of a MIMO antenna for diversity applications is measured in terms of the following parameters:

Envelope correlation coefficient (ECC):

It is calculated by using the scattering parameter values through the standard equation (1)[36]:

$$\rho_e = \frac{|S_{11}^* S_{12} + S_{21}^* S_{22}|^2}{(1 - (|S_{11}|^2 + |S_{21}|^2))(1 - (|S_{22}|^2 + |S_{12}|^2))}. \quad (1)$$

Table 2. Comparison of two antenna configurations with previously reported structures

		Bandwidth		Dimensions			
S. No.	Antenna	GHz	%	mm^2	$\lambda_L \times \lambda_L$	% Size reduction	Diversity
1.	[2]	1.85–11.9	146.18	55 × 100	$0.34\lambda_L \times 0.62\lambda_L$	43.07	**Spatial**
2.	[3]	3.1–10.6	109.49	40 × 60	$0.41\lambda_L \times 0.62\lambda_L$	52.79	
3.	[4]	3.1–10.6	109.49	35 × 40	$0.36\lambda_L \times 0.41\lambda_L$	18.7	
4.	[5]	2.2–13.1	142.48	40 × 66.8	$0.29\lambda_L \times 0.49\lambda_L$	15.55	
5.	[6]	3.1–5	46.91	33 × 35	$0.34\lambda_L \times 0.36\lambda_L$	1.96	
6.	[7]	3.1–12	117.88	33 × 45.5	$0.34\lambda_L \times 0.47\lambda_L$	24.91	
7.	[8]	2.27–10.2	127.19	80 × 60	$0.61\lambda_L \times 0.45\lambda_L$	56.28	
8.	[10]	3.6–17.6	132.08	46 × 27.2	$0.55\lambda_L \times 0.33\lambda_L$	33.88	
9.	[11]	2.5–11	125.93	40 × 50	$0.33\lambda_L \times 0.42\lambda_L$	13.42	
10.	[12]	4.183–6.584	44.60	50 × 80	$0.7\lambda_L \times 1.12\lambda_L$	84.69	
11.	[13]	3.1–10.6	109.49	30 × 42	$0.31\lambda_L \times 0.43\lambda_L$	9.98	
12.	[14]	7.87–12.08	42.21	39 × 17.5	$1.02\lambda_L \times 0.46\lambda_L$	74.42	
13.	**Ant I**	**4.4–51.5**	**168.5**	**17 × 33**	$\mathbf{0.25\lambda_L \times 0.48\lambda_L}$	–	
14.	[16]	3.25–12	114.75	27 × 52	$0.29\lambda_L \times 0.56\lambda_L$	6.34	**Pattern**
15.	[17]	3–11	114.29	34 × 49	$0.34\lambda_L \times 0.49\lambda_L$	8.7	
16.	[18]	2.8–11	118.84	58 × 58	$0.54\lambda_L \times 0.54\lambda_L$	47.84	
17.	[19]	2.76–10.75	118.28	50 × 50	$0.46\lambda_L \times 0.46\lambda_L$	28.12	
18.	[20]	3–12	120.00	80 × 80	$0.8\lambda_L \times 0.8\lambda_L$	76.23	
19.	[22]	2.7 to 10.9	120.59	50 × 45	$0.45\lambda_L \times 0.41\lambda_L$	17.56	
20.	[23]	2.9–10.8	115.33	70 × 80	$0.68\lambda_L \times 0.77\lambda_L$	70.95	
21.	[24]	3.1–12	117.88	46 × 46	$0.48\lambda_L \times 0.48\lambda_L$	33.98	
22.	**Ant II**	**3.8–51.5**	**171.2**	**31 × 31**	$\mathbf{0.39\lambda_L \times 0.39\lambda_L}$	–	

https://doi.org/10.1017/S1759078720000549 Published online by Cambridge University Press

An ECC of 0.5 or −6 dB is the maximum limit for any diversity antenna [37]. Figure 12 presents the ECC values for both diversity configurations. For spatial diversity configuration, ECC ≤ −30 dB is observed across a frequency spectrum of 4–24 GHz. Thereafter, ECC ≤ −40 dB is observed at higher frequencies. In case of pattern diversity configuration, −20 ≤ ECC ≤ −30 dB is achieved between 4 and 12 GHz. After 12 GHz, ECC ≤ −40 dB is observed for every frequency in the operating band.

Diversity gain (DG):

It quantifies the diversity effect on the received signal in a multichannel wireless environment. It can be calculated by replacing time-averaged SNR with cumulative distribution function (CDF) in the difference equation given in [38]. The normally used CDF is 1 or 10% [39, 40]. It is calculated from the above calculated ECC values by using the following relation:

$$\mathrm{DG} = 10\sqrt{1 - |\rho_e|^2}. \tag{2}$$

The calculated values of DG are shown in Fig. 13. It is observed that an almost constant DG is obtained across the entire operating band for each configuration.

Capacity loss, C_{loss}

It quantifies the estimated maximum transmission rate in a communication channel in case of rich multipath environment for reliable transmission. For a MIMO antenna, the maximum value accepted in a MIMO antenna is 0.4 b/s/Hz. It is calculated in b/s/Hz by using correlation matrix (3) [41].

$$C_{\mathrm{loss}} = -\log_2(\psi^R), \tag{3}$$

where ψ^R = correlation matrix of the receiving antenna and is expressed mathematically as

$$\psi^R = \begin{bmatrix} \rho_{11} & \rho_{12} \\ \rho_{21} & \rho_{22} \end{bmatrix}, \tag{4}$$

$$\rho_{ii} = 1 - (|S_{ii}|^2 + |S_{ij}|^2), \tag{5}$$

$$\rho_{ij} = -(S_{ii}^* S_{ij} + S_{ji}^* S_{ij}), \tag{6}$$

$i, j = 1$ or 2.

Figure 14 demonstrates that the capacity loss is <0.4 b/s/Hz for each configuration.

Comparison with other geometries

Table 2 presents that for spatial diversity configuration, a size reduction up to 85% is achieved over previous structures with a fractional bandwidth of ∼169%. In case of pattern diversity configuration, a size reduction of ∼76% is achieved with a fractional bandwidth of 171%.

Conclusion

Two-element spatial and pattern diversity configurations of circular slot-loaded feather-shaped super wideband monopole antenna are investigated for MIMO applications. By using an inter-element separation of $\lambda/10$ in spatial configuration, isolation is improved. In pattern diversity configuration, a diagonal metallic strip is inserted between two orthogonal elements for inter-element isolation improvement. Both configurations have good diversity performance parameters such as ECC, DG, and channel capacity loss. These values of diversity performance parameters, wide bandwidth, and miniaturized dimensions prove the suitability of designed antenna configurations for SWB MIMO applications.

References

1. **Nezhad SMA and Hassani HR** (2010) A novel triband E-shaped printed monopole antenna for MIMO application. *IEEE Antennas and Wireless Propagation Letters* **9**, 576–579.
2. **Lee J-M, Kim K-B, Ryu H-K and Woo J-M** (2012) A compact ultrawideband MIMO antenna with WLAN band-rejected operation for mobile devices. *IEEE Antennas and Wireless Propagation Letters* **11**, 990–993.
3. **Liu XL, Wang Z, Yin Y-Z and Wang JH** (2014) Closely spaced dual band-notched UWB antenna for MIMO applications. *Progress in Electromagnetics Research C* **46**, 109–116.
4. **Zhang S, Ying Z, Xiong J and He S** (2009) Ultrawideband MIMO/diversity antennas with a tree-like structure to enhance wideband isolation. *IEEE Antennas and Wireless Propagation Letters* **8**, 1279–1282.
5. **Patre SR and Singh SP** (2016) Broadband multiple-input–multiple-output antenna using castor leaf-shaped quasi-self-complementary elements. *IET Microwaves, Antennas & Propagation* **10**, 1673–1681.
6. **Zhang S and Pedersen GF** (2016) Mutual coupling reduction for UWB MIMO antennas with a wideband neutralization line. *IEEE Antennas and Wireless Propagation Letters* **15**, 166–169.
7. **Khan MS, Shoaib I, Autizi E, Capobianco A-D, Najam AI and Shafique MF** (2014) Compact ultra-wideband diversity antenna with a floating parasitic digitated decoupling structure. *IET Microwaves, Antennas & Propagation* **8**, 747–753.
8. **Hong S, Chung K, Lee J, Jung S, Lee SS and Choi J** (2008) Design of a diversity antenna with stubs for UWB applications. *Microwave and Optical Technology Letters* **50**, 1352–1356.
9. **Liu J, Esselle KP, Hay SG, Sun Z and Zhong S** (2013) A compact super-wideband antenna pair with polarization diversity. *IEEE Antennas and Wireless Propagation Letters* **12**, 1472–1475.
10. **Dabas T, Gangwar D, Kanaujia BK and Gautam A** (2018) Mutual coupling reduction between elements of UWB MIMO antenna using small size uniplanar EBG exhibiting multiple stop bands. *AEU – International Journal of Electronics and Communications* **93**, 32–38.
11. **Lin G-S, Sung C-H, Chen J-L, Chen L-S and Houng M-P** (2017) Isolation improvement in UWB MIMO antenna system using carbon black film. *IEEE Antennas and Wireless Propagation Letters* **16**, 222–225.
12. **Jehangir SS and Sharawi MS** (2017) A miniaturized UWB biplanar Yagi-like MIMO antenna system. *IEEE Antennas and Wireless Propagation Letters* **16**, 2320–2323.
13. **Yadav D, Abegaonkar MP, Koul SK, Tiwari VN and Bhatnagar D** (2018) Two element band-notched UWB MIMO antenna with high and uniform isolation. *Progress in Electromagnetics Research M* **63**, 119–129.
14. **Chang Y, Liu Q, Tang X, Du G, Li G and Cheng D** (2019) Compact MIMO antenna with high isolation characteristic for UWB portable applications. *Microwave and Optical Technology Letters* **62**, 1391–1397.
15. **Kumar J** (2016) Compact MIMO antenna. *Microwave and Optical Technology Letters* **58**, 1294–1298.
16. **Koohestani M, Moreira AA and Skrivervik AK** (2014) A novel compact CPW-fed polarization diversity ultrawideband antenna. *IEEE Antennas and Wireless Propagation Letters* **13**, 563–566.
17. **Yoon H, Yoon Y, Kim H and Lee C-H** (2011) Flexible ultra-wideband polarisation diversity antenna with band-notch function. *IET Microwaves, Antennas & Propagation* **5**, 1463.

https://doi.org/10.1017/S1759078720000549 Published online by Cambridge University Press

18. **Chacko BP, Augustin G and Denidni TA** (2013) Uniplanar slot antenna for ultrawideband polarization-diversity applications. *IEEE Antennas and Wireless Propagation Letters* **12**, 88–91.
19. **Chacko BP, Denidni TA and Augustin G** (2013) Uniplanar polarisation diversity antenna for ultra-wideband systems. *IET Microwaves, Antennas & Propagation* **7**, 851–857.
20. **Gallo M, Antonino-Daviu E, Ferrando-Bataller M, Bozzetti M, Molina-Garcia-Pardo JM and Juan-Llacer L** (2012) A broadband pattern diversity annular slot antenna. *IEEE Transactions on Antennas and Propagation* **60**, 1596–1600.
21. **Ibrahim AA, Machac J and Shubair RM** (2017) Compact UWB MIMO antenna with pattern diversity and band rejection characteristics. *Microwave and Optical Technology Letters* **59**, 1460–1464.
22. **Femina BS and Mishra SK** (2016) Compact WLAN band-notched printed ultrawideband MIMO antenna with polarization diversity. *Progress in Electromagnetics Research C* **61**, 149–159.
23. **Taha-Ahmed B and Lasa EM** (2018) Polarization diversity UWB antennas with and without notched bands. *Progress in Electromagnetics Research M* **76**, 101–111.
24. **Debnath P, Karmakar A, Saha A and Huda S** (2018) UWB MIMO slot antenna with Minkowski fractal shaped isolators for isolation enhancement. *Progress in Electromagnetics Research M* **75**, 69–78.
25. **Singhal S and Singh AK** (2016) CPW-fed hexagonal Sierpinski super wideband fractal antenna. *IET Microwaves, Antennas & Propagation* **10**, 1701–1707.
26. **Aziz SZ and Jamlos MF** (2016) Compact super wideband patch antenna design using diversities of reactive loaded technique. *Microwave and Optical Technology Letters* **58**, 2811–2814.
27. **Singhal S and Singh AK** (2017) CPW-fed octagonal super-wideband fractal antenna with defected ground structure. *IET Microwaves, Antennas & Propagation* **11**, 370–377.
28. **Rahman MN, Islam MT, Mahmud MZ and Samsuzzaman M** (2017) Compact microstrip patch antenna proclaiming super wideband characteristics. *Microwave and Optical Technology Letters* **59**, 2563–2570.
29. **Figueroa-Torres CÁ, Medina-Monroy JL, Lobato-Morales H, Chávez-Pérez RA and Calvillo-Téllez A** (2017) A novel fractal antenna based on the Sierpinski structure for super wide-band applications. *Microwave and Optical Technology Letters* **59**, 1148–1153.
30. **Yuan B, Zheng YH, Zhang XH, You B and Luo GQ** (2017) A bandwidth and gain enhancement for microstrip antenna based on metamaterial. *Microwave and Optical Technology Letters* **59**, 3088–3093.
31. **Palaniswamy SK, Kanagasabai M, Kumar SA, Alsath MGN, Velan S and Pakkathillam JK** (2017) Super wideband printed monopole antenna for ultra wideband applications. *International Journal of Microwave and Wireless Technologies* **9**, 133–141.
32. **Darimireddy NK, Reddy RR and Prasad AM** (2018) A miniaturized hexagonal-triangular fractal antenna for wide-band applications [antenna applications corner]. *IEEE Antennas and Propagation Magazine* **60**, 104–110.
33. **Raheja DK, Kanaujia BK and Kumar S** (2019.) Low profile four-port super-wideband multiple-input-multiple-output antenna with triple band rejection characteristics. *International Journal of RF and Microwave Computer-Aided Engineering* **29**, 1–13.
34. **Manohar M, Kshetrimayum RS and Gogoi AK** (2015) Super wideband antenna with single band suppression. *International Journal of Microwave and Wireless Technologies* **9**(1), 1–8. doi: 10.1017/S1759078715000963.
35. **Huang Y and Boyle K** (2008) *Antennas From Theory to Practice*. West Sussex, UK: John Wiley & Sons, p. 64.
36. **Blanch S, Romeu J and Corbella I** (2003) Exact representation of antenna system diversity performance from input parameter description. *Electronics Letters* **39**, 705–707.
37. **Najam AI, Duroc Y and Tedjini S** (2009) Design of MIMO antennas for ultra-wideband communications. *MajecSTIC 2009 Avignon*, France, du 16 au 18 novembre 2009.
38. **Taga T** (1990) Analysis for mean effective gain of mobile antennas in land mobile radio environments. *IEEE Transactions on Vehicular Technology* **39**, 117–131.
39. **Flaviis FD, Jofre L, Romeu J and Grau A** (2013) *Multiantenna Systems for MIMO Communications*. San Rafael: Morgan & Claypool Publishers.
40. **Kildal P-S and Rosengren K** (2004) Correlation and capacity of MIMO systems and mutual coupling, radiation efficiency, and diversity gain of their antennas: simulations and measurements in a reverberation chamber. *IEEE Communications Magazine* **42**, 104–112.
41. **Tripathi S, Mohan A and Yadav S** (2015) A compact Koch fractal UWB MIMO antenna with WLAN band-rejection. *IEEE Antennas and Wireless Propagation Letters* **14**, 1565–1568.



Sarthak Singhal was born in Gwalior (M.P.) in 1987. He received his B.E. degree in Electronics & Telecommunication Engineering from SGSITS, Indore (M.P.) in 2010, the M.Tech. degree in Microwave Engineering, and the Ph.D. degree from I.I.T. (B.H.U) Varanasi in 2012 and 2015, respectively. His research areas are microstrip antenna and UWB antennas. He worked as an Assistant Professor at Amity School of Engineering & Technology (ASET), Bijwasan, New Delhi; Amity University, Gwalior, Madhya Pradesh; and Madhav Institute of Technology & Science, Gwalior, Madhya Pradesh. Presently, he is working as an Assistant Professor at Malaviya National Institute of Technology, Jaipur since February 2019. He has published over 40 research papers in journals, 10 in conference proceedings, and two books titled "*Design and Analysis of Shorted Gap Coupled Patch Antenna*" and "*Design and Analysis of Ultra Wideband Microstrip Antennas*" from LAP LAMBERT Academic Publishing House.

https://doi.org/10.1017/S1759078720000549 Published online by Cambridge University Press